

Fittje, Jens; Wagner, Helmut

**Conference Paper**

## Network topography and default contagion in China's financial system

Beiträge zur Jahrestagung des Vereins für Socialpolitik 2020: Gender Economics

**Provided in Cooperation with:**

Verein für Socialpolitik / German Economic Association

*Suggested Citation:* Fittje, Jens; Wagner, Helmut (2020) : Network topography and default contagion in China's financial system, Beiträge zur Jahrestagung des Vereins für Socialpolitik 2020: Gender Economics, ZBW - Leibniz Information Centre for Economics, Kiel, Hamburg

This Version is available at:

<https://hdl.handle.net/10419/224605>

**Standard-Nutzungsbedingungen:**

Die Dokumente auf EconStor dürfen zu eigenen wissenschaftlichen Zwecken und zum Privatgebrauch gespeichert und kopiert werden.

Sie dürfen die Dokumente nicht für öffentliche oder kommerzielle Zwecke vervielfältigen, öffentlich ausstellen, öffentlich zugänglich machen, vertreiben oder anderweitig nutzen.

Sofern die Verfasser die Dokumente unter Open-Content-Lizenzen (insbesondere CC-Lizenzen) zur Verfügung gestellt haben sollten, gelten abweichend von diesen Nutzungsbedingungen die in der dort genannten Lizenz gewährten Nutzungsrechte.

**Terms of use:**

*Documents in EconStor may be saved and copied for your personal and scholarly purposes.*

*You are not to copy documents for public or commercial purposes, to exhibit the documents publicly, to make them publicly available on the internet, or to distribute or otherwise use the documents in public.*

*If the documents have been made available under an Open Content Licence (especially Creative Commons Licences), you may exercise further usage rights as specified in the indicated licence.*

# Network topography and default contagion in China's financial system

Jens Fittje\* and Helmut Wagner<sup>†</sup>

FernUniversität in Hagen

August 12, 2020

The topography of China's financial network is unique. Is it also uniquely robust to contagion? We explore this question using network theory. We find that networks that are more concentrated are less fragile when connectivity is low. However, they remain vulnerable to the occurrence of large-scale default cascades at higher levels of connectivity than a decentralized network. We implement Chinese characteristics into our model and simulate it numerically. The simulations show, that the large state-controlled banks act as effective stopgaps for contagion, which makes the Chinese network relatively robust. This robustness persists even when a medium sized bank defaults.

JEL Codes: E40, E44, G01, G21;

Keywords: Interbank Network; Financial Contagion; China's interbank market; Financial market stability; Complex networks; Network topography;

---

\*Corresponding author. Fernuniversität in Hagen, Macroeconomics. email: jens.fittje@fernuni-hagen.de

<sup>†</sup>Fernuniversität in Hagen, Macroeconomics

# 1 Introduction

In May 2019, the Chinese government took over the struggling Baoshang bank. This was an unusual step; the last government takeover of a bank had at that time been more than two decades ago. The government intervention was caused by the rising liquidity and credit risk in the balance of the Inner-Mongolian city commercial bank. The bank had rapidly expanded its balance in the years prior to the takeover. This expansion created not only a high dependence on interbank funding, but it was also coupled with an inadequate assessment of credit risks. A few month later, the government acted again to rescue a troubled bank, and the rescued bank was again a smaller city commercial bank: The Bank of Jinzhou based in the Liaoning province. This time the government sought to avoid the negative consequences of an outright government takeover. The rescue took the form of a partial bailout by three state-owned asset management companies. The year closed with yet another government intervention, this time to orchestrate the recapitalization of the Shandong based Hengfeng bank, one of China's twelve joint-stock commercial banks. These three very prominent episodes of bank rescues in the span of a few months raised concerns about the business models pursued by China's smaller banks, especially the city commercial banks. The inadequate risk assessment and reckless expansionism may not be unique to the three distressed banks but a characteristic of a significant subset of China's commercial banks. A stress test conducted by the People's Bank of China found indeed, that about 13% of China's smaller banks (City commercial banks, rural and township banks, credit cooperatives) should be classified as high-risk banks.<sup>1</sup>

The isolated failure of a single small bank in itself is not necessarily cause for concern. Its market share would likely be too small to cause significant economic distress. What is concerning about the potential failure of a small bank is the possibility of knock-on effects. The default could be contagious. Contagion seems especially probable in a system

---

<sup>1</sup>Financial Stability Analysis Group of the PBoC (2019)

with a significant subset of struggling banks. Without swift government intervention, contagion and its effect on interbank market liquidity could create a cascade of failures, a cascade that would cause serious economic harm.

For contagion to spread, the failure of a bank must cause other banks to become distressed. The failed bank has to be connected to banks which are vulnerable to the initial failure. The extent of contagion therefore hinges on the number of vulnerable banks that can be reached from the initial failed bank. The size of this vulnerable cluster is not only a function of individual bank balances, but also a function of the financial networks topography. In this paper, we are exploring this aspect of contagion, the impact that network topography has on the frequency and extent of contagion. We analyze in particular the differences in contagion resilience between a decentralized and a more hierarchical/ concentrated network similar to the Chinese financial network.

For this analysis, we make use of the theoretical approach to networks explored by network science/ graph theory to create a model of a financial network. We build in particular on the framework provided by Newman, Strogatz and Watts (2001) and Gai and Kapadia (2010) to derive the effect of changes to the network topography analytically. We additionally conduct numerical simulations of the model to illustrate our analytical results. The simulations are conducted for a generic calibration of the model and for a model calibrated to have key characteristics of the Chinese financial network. We find that the concentration of a network has a significant impact on the spread and frequency of contagion. A concentrated network with a few large hubs, is less prone to widespread contagion, when connectivity is low. It is however more susceptible to significant contagion than a decentralized network without large hubs, when connectivity is high. Networks become immune to contagion at higher levels of connectivity, which is in line with the observations described in Allen and Gale (2000). However, the level of connectivity needed to reach immunity is higher in a concentrated network than in a decentralized network.

The remainder of this paper is constructed as follows: The next section illustrates this paper's place within the research literature in the topic of financial contagion. The third section provides some stylized facts about the Chinese financial network. The analytical derivation is conducted in the fourth section and the numerical simulations can be found in the fifth section. The final section concludes the paper.

## 2 Related Literature

This paper is closely related to the growing body of research concerned with the sources, avenues and effects of contagion within theoretical financial networks. A first thorough theoretical look at contagion in financial networks was provided by Allen and Gale (2000), who analyze the possibility of contagion within different setups of highly stylized complete and incomplete networks. A similar question is at the basis of Eisenberg and Noe (2001). Complex networks have been a research topic in the realm of physics/network science, for some time and this research brought forth important insights into networks, which can be applied to financial networks. Of great importance for this work is the formalization of networks through generating functions described in Newman, Strogatz and Watts (2001). The examination of the World Wide Web and the theoretical framework developed to describe it are also important for the analytical exploration undertaken in this paper. We use in particular the approach to networks with hidden variables as presented in Caldarelli et al. (2002), Boguñá and Pastor-Satorras (2003) and Söderberg (2003) for our analysis. A newer strand of economic literature has adapted the studies of complex networks for the context of financial networks. Gai and Kapadia (2010) and Gai, Haldane and Kapadia (2011) explore the occurrence of contagion and liquidity hoarding in the context of decentralized random networks. A similar question is at the basis of Amini, Cont and Minca (2016) who examine default cascades in the context of a heterogeneous financial network. Nier et al. (2008) analyze the impact of a

tiered financial network on financial stability, without the analytical derivation present in our paper. The question of network structure is also at the heart of Acemoglu, Ozdaglar and Tahbaz-Salehi (2015), who are analyzing the robustness of different regular network structures. The question of efficiency in interbank networks is explored in Castiglionesi and Navarro (2019).

We draw inspiration for our assumptions for the Chinese financial network from the empirical analysis of other financial sectors. In particular from the analysis of the Brazilian financial sector found in Cont, Moussa and Santos (2013) and the analysis of the Italian financial network found in Masi, Iori and Caldarelli (2006). A paper closely related to the topic of the present paper is Sun (2018). They examine the Chinese financial network to quantify systemic risk. Their model is fed with balance sheet data from Chinese large, joint-stock and city commercial banks. This data is used to create a complete regular network using the maximum entropy method. We assume in contrast to this, that the Chinese financial network is a sparse network.

We base our assumption on the Chinese financial network in a large part on the survey of balances of commercial banks. However, we also draw upon the descriptions of developments in the Chinese financial network provided by Xian and Lu (2019) and Xia (2020). We also used the analysis on the Chinese financial network published by the Reserve Bank of Australia in the form of a bulletin on the repo market<sup>2</sup> and a statement on monetary policy on China's small banks.<sup>3</sup> Another source of information are the financial stability reports provided by the People's Bank of China.<sup>4</sup>

---

<sup>2</sup>Reserve Bank of Australia (2017)

<sup>3</sup>Reserve Bank of Australia (2019)

<sup>4</sup>Financial Stability Analysis Group of the PBoC (2019)

### 3 Stylized Facts

Like most sectors of China's economy, the financial sector has seen rapid change in the last decades. The market share of the five largest state-controlled banks<sup>5</sup> has slowly declined in the last two decades and a large amount of new regional city and rural banks as well as private and foreign funded banks have been established. The China Banking and Insurance Regulatory Commission (CBIRC) lists now more than 4000 banks in its register of banks and financial corporations. The list counts five large commercial banks, 12 joint-stock commercial banks and 134 city commercial banks. Most of the banks on the list are small and smallest rural banks and credit cooperatives. The smallest banks including the city commercial banks held about a quarter of all assets of the banking system in 2018, the joint-stock bank a fifth and the largest bank slightly more than a third.<sup>6</sup> Despite the rapid establishment of new banks China's banking sector still remains a very tiered system. The five largest banks enjoy a privileged position, because of their access to a vast pool of deposits from state-backed institutions and corporate payrolls. They also have a greater ability to raise funds from the emission of equity and bonds. The smaller banks on the other hand have to rely more on the interbank market to acquire funds. The effective cap on deposit rates additionally limits the ability to compete for costumers through attractive deposit conditions. Funding costs for the smaller banks are therefore in general higher and they are incentivized to invest in riskier higher yield projects/loans. Because of the spotlight put onto the city commercial banks, we have surveyed the 2018 annual reports of 47 city commercial banks, to develop an understanding of the characteristics of the balance sheets of these banks. We have also looked at the annual reports of the five largest banks, the Postal Savings Bank and 12 joint-stock commercial banks. Figure (1) shows the distribution of funding for the different categories of banks. Outside of the sheer size difference between the joint-

---

<sup>5</sup>Bank of Communications, Industrial and Commercial Bank of China, Bank of China, China Construction Bank and China Agricultural Bank

<sup>6</sup>Reserve Bank of Australia (2019), p.21.

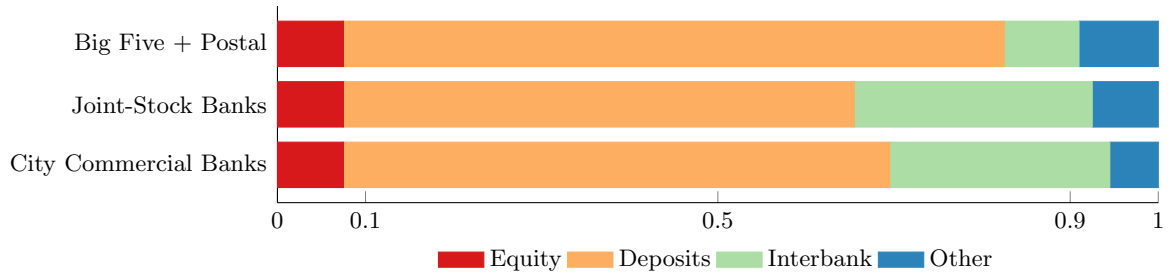


Figure 1: Funding Sources

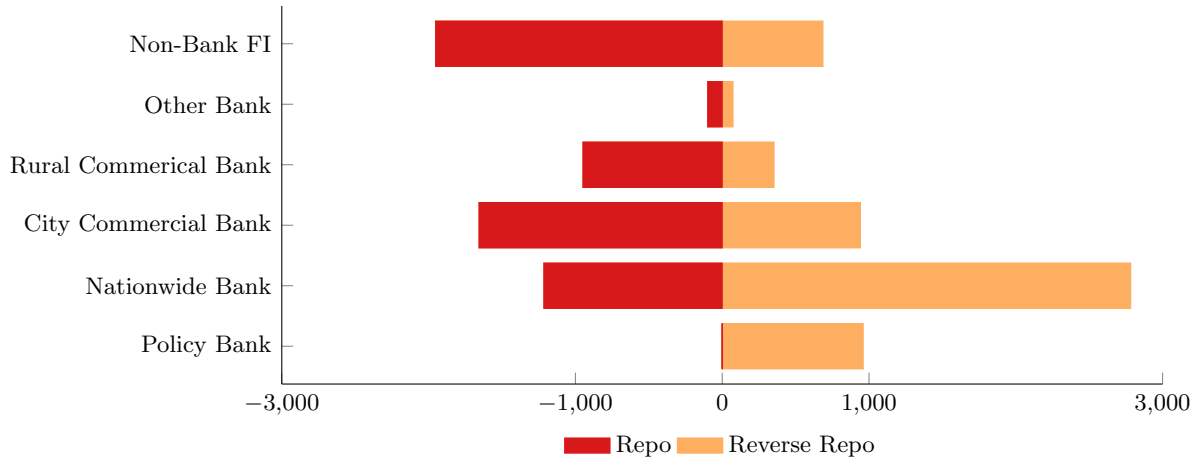


Figure 2: Pledged Repo Market

stock commercial banks and the city commercial banks, their balances are on average similar. The large commercial banks differ from the smaller banks not only in size, but also in the composition of their balances. The fraction of funding that the largest banks obtain from the interbank market is on average smaller. The largest banks fund on average 10% of their balance through the interbank market (including repurchase agreements and certificates of deposit), whereas the joint stock banks fund 29% and the city commercial banks 26% through the interbank market. The average equity ratio of the banks is 7.5% for the city commercial and large banks and 7% for the joint-stock banks (excluding the Hengfeng Bank which posts negative equity for 2018 in its 2019 annual report).

Another aspect of China's tiered banking system expresses itself quite clearly in the



statistics of the market for pledged repurchase agreements. Figure (2) shows a breakdown of the market according to institution type. The large nationwide banks and the policy banks are net providers of liquidity, while the city commercial banks are net receivers of liquidity. The easier access to liquidity from outside the interbank market that the large banks enjoy destines them to become net lenders on the interbank market.

These observations paint the picture of a tiered financial network, a network that has characteristics of a core-periphery structure as remarked by Sun (2018). This core-periphery structure may however differ from the core-periphery structure found in other financial networks.<sup>7</sup> A very distinct feature of the Chinese financial market is the low percentage of funds that the large banks source from the interbank market. This facilitates a one-sided market structure, where the large banks act as net-providers of liquidity and the smaller banks as net-receivers of liquidity.

## 4 Model

In this section we develop the theoretical framework to highlight the impact of changes in the network topography on the probability of widespread contagion. First we give an abbreviated overview over the framework developed by Newman, Strogatz and Watts (2001) and Gai and Kapadia (2010) and the phenomenon of phase transitions in networks. We then use these building blocks to show how a change in topography changes the occurrence of a phase transition. This theoretical exploration cannot only yield interesting observations about the robustness of core-periphery financial networks in general. The exploration can also give insight into the impact that the structure of the Chinese financial network has on financial stability and the consequences of deeper integration of the smaller Chinese banks into the interbank market.

Network science, which is also referred to as graph theory, has in the last decades

---

<sup>7</sup>as described in for example Cont, Moussa and Santos (2013)

become a well-established tool in the analysis of financial networks, starting with the seminal works of Allen and Gale (2000). In graph theory, the financial network can be represented as a collection of nodes and links connecting the nodes. Usually these links have a direction, so that the link from node  $a$  to node  $b$  is not identical to the link from node  $b$  to node  $a$ . The nodes of the graph are the participants/ banks in the financial network and the links are the claims existing in the network. In practice, every contract would form a new link between two banks, with its own maturity, volume and seniority. In graph representations of financial networks it is common and convenient to bundle all claims from one bank on another into a single link. It is also clear that unlike other graphs, there can be no claims of a bank on itself. Another analytical simplification is to disallow the netting of claims, so that a link from  $a$  to  $b$  can exist at the same time as a link from  $b$  to  $a$ . The resulting graph of a financial network is a simple weighted digraph without self-loops.

Most real world networks are sparse. Only a fraction of the links that could theoretically exist in a network actually exist at any given time. The question of how many of the possible links exist and more importantly, which links exist, is crucial for the assessment of the potential for contagion in the network. We will discuss theoretical approaches to the question of which links are present later on, but first we take a closer look at the elements of the digraph and vulnerable banks.

#### 4.1 Digraph and banks

Modeling the financial network as a simple digraph without netting of claims limits the maximum number of theoretically possible links. Let an oriented link from node  $a$  to node  $b$  represent a debt of node  $a$  owed to node  $b$ , then two nodes can only be connected by two links, a link going from node  $a$  to node  $b$  and one from  $b$  to  $a$ . If we set  $L$  as the number of links and  $N$  as the number of nodes in the graph (the number of banks in the financial network), then the maximum number of possible links is limited

to  $L_{max} = (N - 1)N$ . The number of links ending at a node is the node's in-degree  $j$  and the number of links starting at a node is its out-degree  $k$ . The probability distribution  $p_j$  is the fraction of nodes with an in-degree of  $j$  and the probability distribution  $p_k$  is the fraction of nodes with an out-degree of  $k$ . We can also express  $p_k$  as  $p_k = \frac{N_k}{N}$  and  $p_j$  as  $p_j = \frac{N_j}{N}$ . The fraction of nodes with in-degree  $j$  and out-degree  $k$  is captured by  $p_{jk}$ , the joint degree distribution of in- and out-degree. Newman, Strogatz and Watts (2001) highlight, that this distribution in general is not equal to the product of the distributions of in- and out-degrees,  $p_{jk} \neq p_k p_j$ .  $p_j$  and  $p_k$  can be correlated, so that nodes with high in-degrees also have high out-degrees. This is likely the case in the core-periphery financial networks described by Masi, Iori and Caldarelli (2006) and Cont, Moussa and Santos (2013).

Let  $i \in \{1, \dots, N\}$  be a bank in the financial system. The stylized balance of bank  $i$  is composed of two categories of assets, two categories of liabilities and equity. The assets are fixed Assets  $A_i^f$  and interbank assets  $A_i^b$ .  $A_i^f$  represent (illiquid) assets of the bank that are exogenous to the interbank market, such as commercial and retail loans, non-financial bonds, deposits with the central bank and other assets.  $A_i^b$  represent assets such as loans to other financial intermediaries, certificates of deposits and other kinds of interbank assets. The liabilities are liabilities exogenous to the interbank market  $D_i$  and interbank liabilities  $L_i^b$ .  $D_i$  represents liabilities such as deposits.  $L_i^b$  represents the same instruments as  $A_i^b$  viewed from the side of the debtor. A corresponding asset in the interbank market matches every interbank liability, so that the net interbank assets of the entire market are zero. Banks are also allotted a random amount of equity.<sup>8</sup> In the bank's balance the equity is the difference between the bank's assets and liabilities or  $K_i = A_i^b + A_i^f - D_i - L_i^b$ . Equity serves as an indicator for the solvency of a bank. If the default of an asset or a string of assets results in zero or negative equity, the bank

---

<sup>8</sup>We follow Gai and Kapadia (2010), p. 2407, with this random allotment of equity. This is however only valid for the analytical part of the paper. For the numerical simulations of the generic model, we attribute an equal amount of equity to every bank.

fails. A bank that fails defaults completely on all of its interbank liabilities and leaves the network. This zero recovery assumption is a common assumption when modeling contagion in interbank networks.<sup>9</sup> From this, it is clear that the vulnerability of a bank to contagion is dependent upon the size of the bank's exposure to a defaulted bank and its equity. It is only vulnerable if there exists a single exposure that surpasses its current equity. Let  $\phi$  be the fraction of interbank assets that have defaulted and  $q$  the resale price of the fixed asset, then the bank will become insolvent if <sup>10</sup>

$$(1 - \phi)A_i^b + qA_i^f - L_i^b - D_i < 0 \quad (1)$$

Which can also be expressed as

$$\phi > \frac{K_i - (1-q)A_i^f}{A_i^b}, \text{ for } A_i^b \neq 0 \quad (2)$$

Gai and Kapadia (2010) simplify their model by assuming, that a bank's interbank assets are distributed evenly among all of its debtors. Which implies that the relative weight of an incoming link decreases when the in-degree of a node increases. This integrates the benefits of diversification into the model.<sup>11</sup> The vulnerability of a bank to the default of a single neighbor can therefore be captured by the following condition

$$\frac{K - (1-q)A^f}{A^b} < \frac{1}{j} \quad (3)$$

It follows from the assumption of a random equity allotment that the probability  $v_j$  of a bank with in-degree  $j$  being vulnerable can be expressed by the equation

$$v_j = P \left[ \frac{K - (1-q)A^f}{A^b} < \frac{1}{j} \right]; \forall j \geq 1 \quad (4)$$

---

<sup>9</sup>Gai and Kapadia (2010), p.2407.

<sup>10</sup>Gai and Kapadia (2010), p.2407.

<sup>11</sup>Gai and Kapadia (2010), p.2406.

## 4.2 Phase transition and generating functions

The number of links in many real world networks remains substantially below the number of theoretically possible links  $L_{max}$ . These networks are sparse. Consequently not every node is connected with every node and the network has clusters of connected nodes. Some of these clusters may be vulnerable clusters. A cluster is vulnerable, when the default of a node within the cluster or of a neighbor of the cluster can trigger a cascade of defaults through the entire cluster. The average size of vulnerable clusters is consequently crucial for the possibility and extent of contagion. If a defaulted bank has no contagious link to a cluster of vulnerable nodes, contagion cannot spread. If the size of the vulnerable cluster is small, then contagion will die out quickly and affect only a few nodes. The average size of the connected clusters depends on the amount and distribution of the links in the network. In a network with no links, there are no connected clusters and consequently no contagion. If the number of links is increased, a point can be reached at which a giant connected cluster of nodes emerges. This point is the phase transition of the network, where it turns figuratively from a gaseous state to a more densely connected liquid state. The phase transition is also of great importance for the occurrence of contagion, as a network-wide contagion cascade is only possible when a giant connected component of vulnerable nodes exists. Newman, Strogatz and Watts (2001) use generating functions to model the probability distributions of a network. This approach allows them to discern key characteristics of a network without the need to define the probability degree distributions. They introduce the following function for the generating function of the joint probability distribution  $p_{jk}$  of a random digraph

$$G(x, y) = \sum_{jk} p_{jk} \cdot x^j \cdot y^k \quad (5)$$

where  $x$  and  $y$  are two independent variables.  $p_{jk}$  is assumed to be correctly normalized, so that if we set  $x = y = 1$  then

$$G(1, 1) = 1 \quad (6)$$

Let  $z$  be the average in-degree, which is given by

$$z = \left. \frac{\delta G}{\delta x} \right|_{x,y=1} = \sum_{jk} j \cdot p_{jk} \quad (7)$$

Every incoming link is also an outgoing link, the average in-degree is accordingly equal to the average out-degree and the net average number of incoming links is zero.<sup>12</sup> Gai and Kapadia (2010) insert the probability that a node is vulnerable  $v_j$  into the generating function to create the generating function for a vulnerable node

$$G(x, y) = \sum_{jk} v_j \cdot p_{jk} \cdot x^j \cdot y^k \quad (8)$$

It follows that  $G(1, 1)$  is no longer one, but given by the equation

$$G(1, 1) = \sum_{jk} v_j \cdot p_{jk} \quad (9)$$

The single-argument generating function  $G_0(y)$  can be defined for the out-degree of a randomly chosen vulnerable bank

$$G_0(y) = G(1, y) = \sum_{jk} v_j \cdot p_{jk} \cdot y^k \quad (10)$$

$G_0(1)$  is equal to  $G(1, 1)$  and yields the fraction of vulnerable nodes in the network. Starting from the single argument generating function for the out-degree, a single argument generating function  $G_1(y)$  for the number of links leaving a node by following a randomly chosen incoming link can be defined. The generating function for the number

<sup>12</sup>Newman, Strogatz and Watts (2001), p.9.

of links that leave a vulnerable neighbor of a randomly chosen bank is captured by the equation

$$G_1(y) = \frac{G'_0(y)}{G'_0(1)} = \frac{\sum_{jk} v_j \cdot j p_{jk} \cdot y^k}{\sum_{jk} j \cdot p_{jk}} \quad (11)$$

The *vulnerable cluster* of the network is the set of vulnerable nodes, which can be reached by following a randomly chosen outgoing link from a vulnerable bank to its end and then to every other vulnerable node reachable from that end. The size and distribution of the vulnerable cluster characterizes how default spreads across the network after an initial failure.<sup>13</sup>

Gai and Kapadia (2010) formulate a generating function for the probability of reaching an outgoing vulnerable cluster of given size, defined as  $H_1(y)$ . They assume that the outgoing links of the defaulting node are tree like. An assumption that is not applied in the numerical simulation. The implicit form of this function is given as

$$H_1(y) = 1 - G_1(1) + yG_1(H_1(y)) \quad (12)$$

The implicit form for the size of the vulnerable cluster a randomly chosen node belongs to is generated by

$$H_0(y) = 1 - G_0(1) + yG_0[H_1(y)] \quad (13)$$

The two equations above can be used to obtain the average vulnerable cluster size  $S$ , which is given by

$$S = H'_0(1) \quad (14)$$

Through substitution this equation can be expressed as

$$S = G_0(1) + \frac{G'_0(1)G_1(1)}{1 - G'_1(1)} \quad (15)$$

---

<sup>13</sup>Gai and Kapadia (2010), p.2409.

Similar to the observation by Newman, Strogatz and Watts (2001), Gai and Kapadia (2010) highlight that the phase transitions at which the average vulnerable cluster size diverges occurs when

$$G'_1(1) = 1 \tag{16}$$

which after substitution becomes

$$z = \sum_{jk} j \cdot k \cdot v_j \cdot p_{jk} \tag{17}$$

The term  $G'_1(1)$  is the average number of outgoing links ending at vulnerable nodes of a vulnerable first neighbor. When this average is below one, the vulnerable clusters are small and contagion cannot spread far. Should the average be above one, then a giant cluster of vulnerable nodes occupying a finite fraction of the network exists, and contagion can spread far. A contagious cascade through the entire network is possible. Gai and Kapadia (2010) state, that there are either two solutions for equation 17 or none. If there are two solutions, there are also two phase transitions and a continuous window of values for  $z$  for which contagion is possible. When  $z$  is below the lower phase transition, the term  $\sum_{jk} jkp_{jk}$  is too small and there are not enough connections in the network for contagion to spread. When  $z$  is above the upper phase transition, then the term  $v_j$  is too small and contagion is inhibited by the absence of vulnerable banks.

### 4.3 Topography and phase transition

The links shape the topography of the network. The decision-rule that governs the presence or absence of a link is therefore of great importance for the network topography and the possibility and extent of contagion. A straightforward approach to establish the presence of links is the use of data from real financial networks. When comprehensive information on the claims existing between the participants of the interbank market is available, a network with a data-driven topography could be constructed. Studies



based on such a detailed set of data have been conducted for example for the Italian and Brazilian interbank markets.<sup>14</sup> These studies found that the respective financial networks have a core-periphery topography. A small core of very well connected banks characterizes this structure. These core-banks are surrounded by a periphery of banks, which are connected to the core but only have sparse connection to other peripheral banks.

Such a data-driven approach can provide important insights into the vulnerabilities of existing networks, but this approach cannot be used for the exploration of the impact of changes in network topography and the number of links on the robustness of the network. In order to explore the effect of these changes, we need to formulate the decision-rule governing link presence.

As noted previously, most real world networks are sparse. From the entirety of possible links only a fraction are present in the network. The decision-rule describes accordingly a process that draws a certain number of links from the distribution of possible links. We assume, that this process is random or more precisely, that the presence of a link is based on that link's probability to be present. We define  $\pi_{a,b}$  as the independent connection probability with which the link connecting node  $a$  with node  $b$  is present in the network. In the directed graph this is the probability that a link starting at node  $a$  and ending at node  $b$  exists.

A special type of network is an Erdős-Renyi graph. This well studied graph has several interesting characteristics. The connection probability for all links is equal. The probability degree distributions ( $p_k$  and  $p_j$ ) are accordingly binomially distributed, which can be approximated by a Poisson distribution for high  $N$ . In a directed Erdős-Renyi graph, there is no correlation between in- and out-degree. Another characteristic is the absence of large hubs – the actual in- and out-degree of the nodes oscillates around the average degree  $z$ .<sup>15</sup>

---

<sup>14</sup>Masi, Iori and Caldarelli (2006) and Cont, Moussa and Santos (2013)

<sup>15</sup>Newman (2002)p.4-6.

Specifically the absence of large hubs in the Erdős-Renyi graph is at odds with the topography of the observed real world financial networks found in Masi, Iori and Caldarelli (2006) and Cont, Moussa and Santos (2013). We use this graph and its topography as a benchmark for the exploration of the effects of changes in network topography on network vulnerability to contagion. It could be interpreted as a completely decentralized financial network. The core-periphery topography of the observed networks can be approximated, when the node degrees are distributed according to a power law.

What shape must the connection probability distribution have, to allow for power law distributed node degrees? In a financial network with a core-periphery topography, some links have a higher connection probability. The core banks have a higher probability of links attaching to them, than the peripheral banks. A conceptual approach to this higher attachment probability has been formulated by Bianconi and Barabasi (2001) and Caldarelli et al. (2002). They capture this higher probability with the introduction of node fitness. Node fitness is an intrinsic attribute of every node, which captures the node's ability to form new links. A node's fitness can be drawn from a pre-defined distribution or a discrete sequence.

The presence of higher fitness nodes is a phenomenon observed in many real world networks. In a financial network, fitness could be generated by a variety of different node attributes. The most obvious is bank size. A larger bank that has a large interbank market presence is bound to attract more links than a smaller bank. Most of its creditors/lenders will be of smaller size and therefore only capable to absorb some of the funds offered/ borrowed by the large bank. Second and often related to bank size is the interbank market position of the bank. Some banks have a privileged position in the market, making them desirable counterparties in the interbank market. Some banks may be perceived as particularly credit worthy or they may have a privileged access to liquidity, like China's large state-controlled banks.

Caldarelli et al. (2002) show that the distribution of node-fitness shapes the probability

degree distribution. A power law distribution of node-fitness will result in a power law distribution of the probability degree distribution. A simple form for a power law distributed sequence of node-fitness is a Pareto distribution, captured in the equation below, where  $n_i$  is the fitness of node  $i$ ,  $a$  is the shape parameter of the Pareto distribution and  $c$  is a constant

$$n_i = c \cdot i^{-(a)} \quad (18)$$

Caldarelli et al. (2002) show that the graph resulting from a power law distributed fitness distribution will also be power law distributed. The distribution of the in-degree can be approximated by

$$p_j \sim j^{-(1+\frac{1}{a})} \quad (19)$$

This highlights the importance of the shape parameter for the topography of the generated network. The parameter also has a role in the occurrence of the phase transition.

Assume that there is a simple undirected graph, which contains some fraction of nodes that are red. The probability of a node being red is the number of red nodes divided by the number of all nodes  $r = \frac{N_r}{N}$ . The generating function for the probability degree distribution of a red node is captured by the equation

$$G_0(x) = \sum_j r \cdot p_j \cdot x^j \quad (20)$$

The average degree in the undirected graph is given by

$$G'_0(1) = \sum_j j \cdot p_j = z \quad (21)$$

Similar to the directed graphs discussed in the previous section, a giant connected cluster of red nodes occurs when  $G'_1(1) = 1$ . For the red nodes in the undirected graph

the equation is

$$G'_1(1) = \frac{1}{z} (G''_0(1)) = \frac{1}{z} \sum_j r \cdot j(j-1)p_j \quad (22)$$

Using equation (19) the following condition for the occurrence of a giant cluster of connected red nodes in a power law distributed undirected graph can be obtained

$$z = \sum_j r \cdot j \cdot (j-1) \cdot j^{-(1+\frac{1}{a})} \quad (23)$$

After some transformation it can be seen, that the right-hand-side of this equation is increasing when  $a$  is increasing. The average degree needed for the network to experience the emergence of a giant connected cluster grows as the fitness distribution's steepness increases.

$$z = \sum_j r \cdot \left( j^{(1-\frac{1}{a})} - j^{-\frac{1}{a}} \right) \quad (24)$$

$$\lim_{a \rightarrow \infty} \sum_j r \cdot \left( j^{(1-\frac{1}{a})} - j^{-\frac{1}{a}} \right) \approx \sum_j r \cdot (j-1) \quad (25)$$

This result is intuitively convincing. Imagine a small simple graph of initially unconnected nodes, of which some are randomly labeled as red nodes. We add links, which we draw at random from a steep fitness distribution, to this graph. Likely we will draw the links connecting the nodes with the highest fitness first. Only when these links are already drawn, will we connect the low fitness nodes. This creates a core-periphery network as long as the total number of links remains below  $L_{max}$ . The average degree needed to reach a high probability for the emergence of a giant connected cluster of red nodes increases in comparison to the Erdős-Renyi graph.<sup>16</sup>

This result can be transferred with some caveats to the directed graph of a financial network discussed in the previous section (4.2). This caveat stems mostly from the fact

---

<sup>16</sup>In the case of an exceptionally steep fitness distribution, the network may first connect every node with one central node. If this central node is not red, no connected cluster of red nodes can form before enough links exist in the network to connect all nodes with the central node.

that we have to formulate an explicit form for the joint-degree distribution  $p_{jk}$ . As noted previously,  $p_{jk}$  is in general not equal to the product of the degree distributions. In particular, if both degree distributions are fed by the same fitness distribution, they should be correlated. In the specific case where the distributions are uncorrelated, we can assume that the joint-degree distribution is simply the product of the degree distributions. If we let for example, the in-degree distribution be a power law distribution, given by  $p_j = j^{-(1+\frac{1}{a})}$  and the out-degree be distribution a binomial distribution, given by  $p_k = \binom{N}{k} \pi_k^k (1 - \pi_k)^{N-k}$ , then the joint-degree distribution is the product of these uncorrelated distributions given by

$$p_{jk} = p_j \cdot p_k = j^{-(1+\frac{1}{a})} \cdot \binom{N}{k} \pi_k^k (1 - \pi_k)^{N-k} \quad (26)$$

If we insert the in-degree distribution into the equation for the average number of outgoing edges ending at vulnerable nodes of a vulnerable first neighbor (17) we obtain the following equation

$$z = \sum_{jk} j \cdot k \cdot v_j \cdot p_{jk} = \sum_{jk} k \cdot v_j \cdot p_k \cdot j^{-\frac{1}{a}} \quad (27)$$

The right-hand-side of this equation is c.p. increasing when the shape parameter is increased. This result is also confirmed by the numerical simulations conducted further on. Furthermore, the numerical simulations suggest that this shifting of the phase transition also occurs when the degree distributions are correlated. The window for the occurrence of system wide contagion is shifted to the right and widened. This result is congruent with intuition. In a core-periphery network, edges are first formed between the core nodes. These high-degree nodes are then very well diversified and unlikely to be vulnerable. The network has to reach a higher average degree than an Erdős-Renyi graph, to facilitate the formation of links between peripheral nodes. But when these links form, it is very probable that the connected peripheral nodes have a low in-degree. These nodes are therefore badly diversified and vulnerable, there is a correlation between

node fitness and vulnerability. The vulnerable cluster forms in the periphery. Network-wide contagion is possible when the erosion of the cores equity through the successive default of peripheral nodes turns core nodes into vulnerable nodes.

## 5 Numerical Simulations

In the following section, we illustrate the analytical results of the previous section through numerical simulations. We will first describe the algorithm used in the generation of the random graphs and then the calibration of the model. The model is calibrated in two different ways: a generic calibration and one that uses Chinese data. The calibrated model is then simulated and we discuss the results of these simulations.

### 5.1 Algorithm and calibration

The algorithm used in the numerical simulations uses hidden variables for the generation of the network. We accordingly first generate the fitness/ hidden variable attributed to each node. This fitness reflects the ability of an individual bank to establish connections with other banks. The fitness of node  $i$  is generated as follows, where the left-hand-term is a simple power law distribution with the constant  $C = 1/(i^a)$  and the shape parameter  $a$ .<sup>17</sup>

$$n_i = C \cdot i^{(-a)} \tag{28}$$

The second step in the algorithm is to calculate the connection probabilities  $\pi_{(i,j)}$  for the existence of a link from node  $i$  to node  $j$ . The calculation of  $\pi_{(i,j)}$  can either be based on the fitness of the end and start node, or on only the fitness of one of the nodes. The

---

<sup>17</sup>The simulation results are relatively robust to different value choices for the constant.

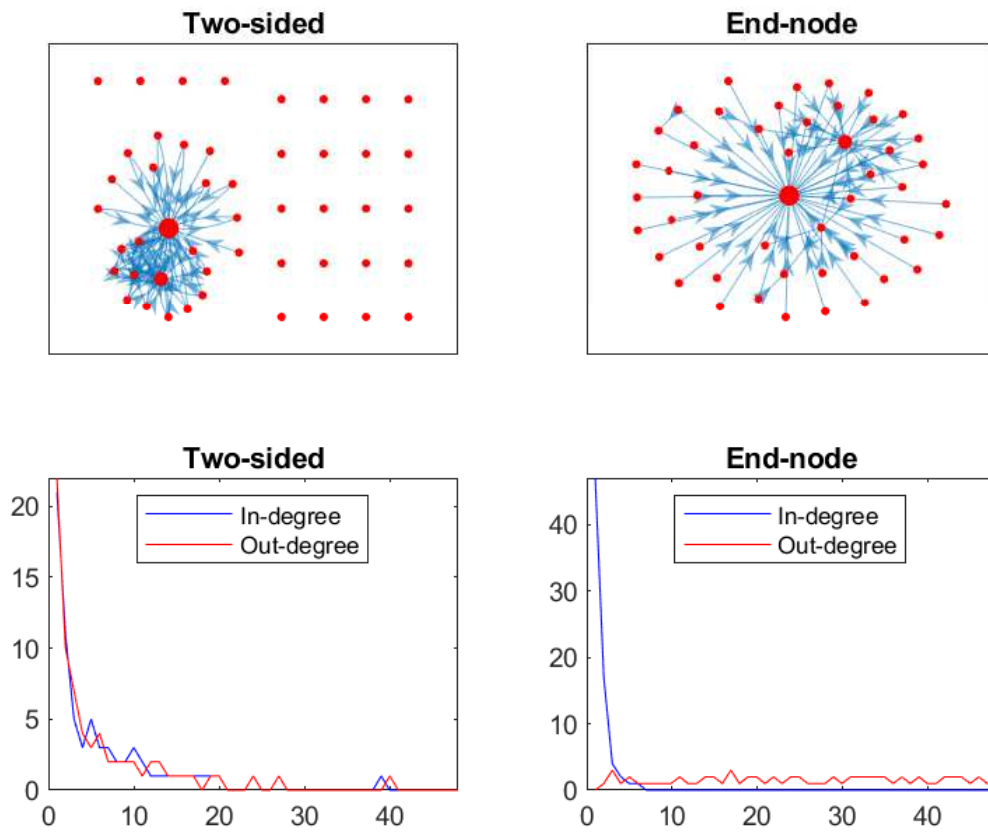


Figure 3: Sample network topographies with 48 nodes resulting from the two-sided and the end-node method for the calculation of the connection probabilities. The shape parameter is 4 for both. The bottom graphs show the degree distribution. Note that the two-sided method leads to a power law distribution of the in- and out-degree, while the end-node method only leads to a power law distribution for the in-degree. The out-degree is binomial distributed.

equation for the calculation of  $\pi_{(i,j)}$  when start- and end-node fitness are used is

$$\pi_{i,j} = \frac{n_i \cdot n_j}{\sum_i n_i}. \quad (29)$$

In the case where only one of the node's fitness is used this equation simply becomes

$$\pi_{i,j} = \frac{n_i}{\sum_i n_i}. \quad (30)$$

The network topography generated by both methods diverges with higher values of the shape parameter. To exclude self-loops, we set  $\pi_{i,i} = 0$ . We use the two-sided method and the method based on the fitness of the end-node in our simulation. The two-sided method generates a core-periphery network, with a very densely interconnected core and a sparsely connected periphery. This reflects the structure of financial networks found in the empirical studies of real world financial networks. The end-node method on the other hand generates a star-shaped network when the shape parameter is high. A star, where a central node acts as the lender to a large periphery of nodes, which are connected to the center but have only sparse connections to other peripheral nodes. This structure reflects a very hierarchical market setup, where the core banks are primarily lenders, whereas the peripheral banks have a larger dependence on interbank funding. Figure (3) shows two sample networks generated with the same shape parameter and average degree and different connection probability calculation methods. The dense core-periphery topography with many unconnected nodes generated by the two-sided method can be clearly seen, as well as the more star shaped topography generated by the end-node method.

In the third step the connection probabilities are used to create an  $N \times N$  connection probability matrix. This matrix contains the connection probability for all possible directed links in the network. We draw a link at random from this matrix and set the



probability of the drawn links to zero. We repeat this until the number of links drawn is equal to the pre-defined value for the total number of links  $L$ . We populate our network with 256 initially solvent banks. For the first simulations, all banks are equal. They all are equipped with the same amount of equity and have the same interbank exposure. The initial interbank assets are set to 20% of the banks' assets and the initial equity is set to 5%. The remaining 80% of the asset-side are non-bank fixed assets. The interbank liabilities are derived endogenously in the model. The difference between liabilities + equity and assets is filled with deposits. With this calibration it is implied, that at the start of the simulation only a bank with four or less incoming links is vulnerable.

For the simulation, we first choose a value for the shape parameter. We conduct simulations for a shape parameter of 0, 1/4, 1 and 3 (or 2 in the case of the end-node simulation). We then iterate the average degree  $z$  from zero to 10. The average degree determines the total number of links in the network. For every value of  $z$ , we draw 4000 different realizations of the network. In every single realization of the network, a single random bank is initially set as insolvent. This bank defaults on all of its interbank liabilities and can trigger default contagion, if it has one or more vulnerable neighbors. A vulnerable neighbor that becomes insolvent also defaults on its interbank liabilities and propagates the contagion further through the network. Every instance of a realization that leads to a significant number of defaults (more than 5%) is counted as an instance of a systemic financial crisis. Over the course of the simulation for a given shape parameter, we then observe the frequency of the occurrence of a systemic financial crisis (the fraction of realizations that result in a crisis) and the extent of the crisis (the fraction of banks that become insolvent when a crisis occurs) for every value of the average degree.

The next step in the numerical simulation is the implementation of key characteristics of the Chinese financial network into our model. We include three different tiers of Chinese banks into our model: the 5 large commercial banks, the 12 joint-stock commercial banks and the 134 city commercial banks, resulting in a network with 151 nodes.

According to the CBIRC, about 40% of the assets of the Chinese banking sector were held by the large banks, 20% by the joint stock banks and between 13 to 14% by the city commercial banks (which we set at 13.4% for arithmetic convenience). We use these asset percentages to create a fitness distribution, where each large bank has a fitness value of 8, each joint stock bank a fitness value of 1.6 and each city commercial bank a value of 0.1. The next step is to calculate the interbank assets and equity of each node. To reflect the size difference in our model, we use the asset share of the different bank tiers for the calculation of the interbank assets. We assume that all banks hold 20% of their assets as interbank assets. The interbank assets of a large bank are then 1.6 units, those of a joint stock bank are 0.32 and of a small bank are 0.02. We set the equity of the large banks and small banks at 7.5% of their assets, and the equity of the joint stock banks at 7%. We simulate two scenarios, one where a random small bank defaults initially and one where a random joint-stock bank defaults initially.

The fitness sequence is fixed, therefore we do not iterate the model over different shapes of the fitness distribution. The average degree of the network is iterated from zero to 10. The simulation draws 4000 realizations for every value of the average degree.

## 5.2 Simulation results

Figure (4) shows the frequency and extent of contagion for four different values of the shape parameter, when the end-node method is used to calculate the connection probability. The curves of the simulation with a shape parameter of zero show the frequency and extent of contagion in an Erdős-Renyi graph. The results are similar to the results obtained by Gai and Kapadia (2010). They show the robust-yet-fragile nature of the financial network, when the average degree is near but below the upper phase transition. The probability for the occurrence of a systemic financial crisis is very low, but the extent of contagion when a crisis occurs is system-wide. The default cascade encompasses the entirety of the financial network. The curves of the simulation with

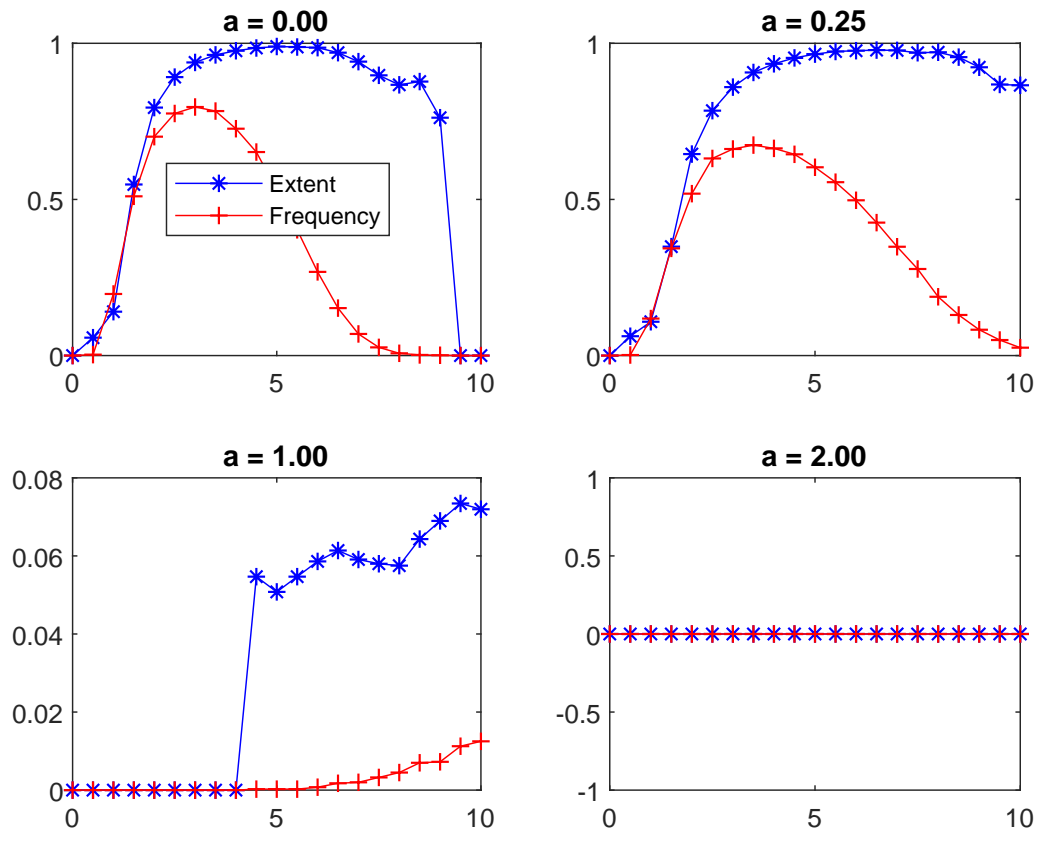


Figure 4: These graphs show the averages for the extent and frequency of a systemic crisis for 4000 iterations of the generic model with different values for the shape parameter, using the end-node method.

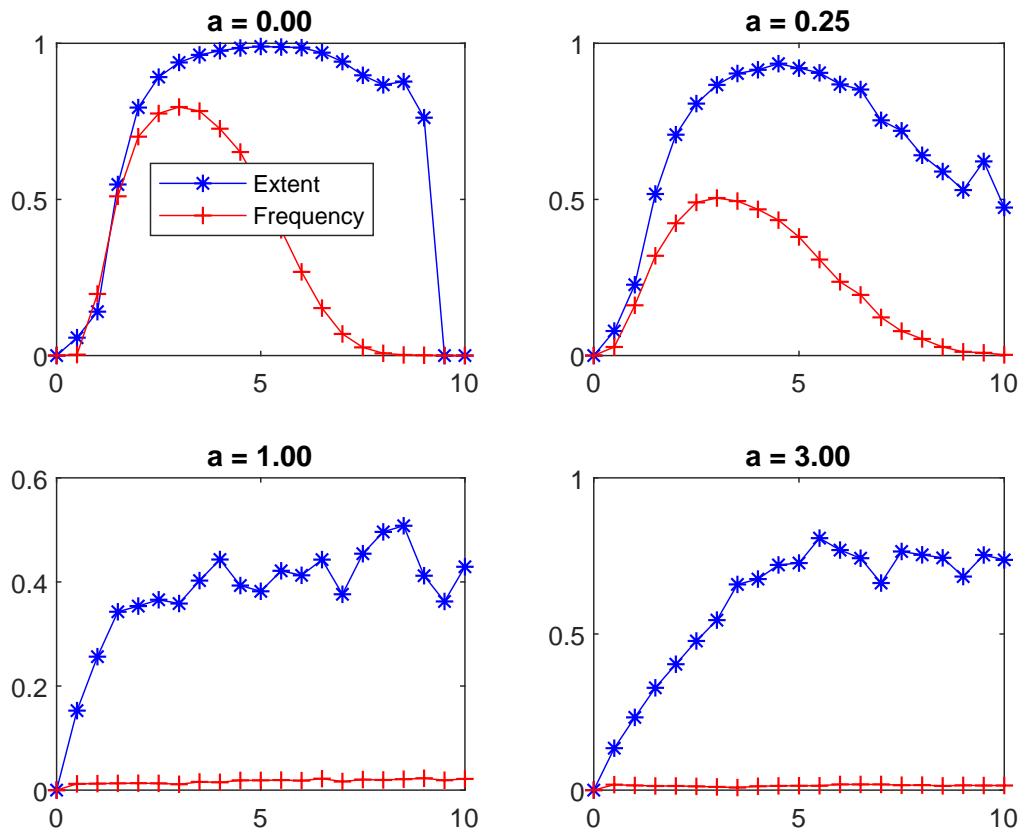


Figure 5: These graphs show the averages for the extent and frequency of a systemic crisis for 4000 iterations of the generic model with different values for the shape parameter, using the two-sided method.

a shape parameter of  $1/4$  and  $1$  validate our analytical expectation of the behavior of the phase transition. The lower phase transition for the occurrence of a giant cluster of vulnerable banks shifts to the right. This is in particular visible for the simulation with a shape parameter of one. The extent of contagion is insignificant below an average degree of five. The upper phase transition also shifts to the right, so that the network remains in the robust-yet-vulnerable state at a significantly higher average degree. The occurrence of the upper phase transition is above the maximum average degree of the numeric simulations. What may not be as clear in 4 as it has been for us during a multitude of test runs, is that the topographies with higher shape parameters also do not self-average themselves as strongly as the Erdős-Renyi topography. The size of the vulnerable cluster varies significantly more between the iterations of the model. We also know from further simulations, that the simulation with a shape parameter of two has a phase transition, where it becomes vulnerable. Another aspect is the extent of contagion. From the simulations it can be observed, that the extent of contagion is lower for the more concentrated topographies. This is likely an effect of the higher number of unconnected nodes in the network. An unconnected node is by definition immune and the share of unconnected nodes is higher in the more concentrated networks. The share of nodes with only an outgoing link is also higher in these networks at higher average degrees. These nodes are also immune to contagion.

Figure (5) shows the results of the simulation for the simulation with networks generated by the two-sided algorithm. The simulation results also show a shift of the upper phase transition. It is however notable, that the shift of the lower phase transition is less pronounced. The maximum extent of contagion occurring in the simulation is also more limited than in either the Erdős-Renyi and the end-node simulation. This is likely the result of the high number of unconnected nodes that persist even at higher average node degrees. Unlike the star-shaped form generated by the end-node algorithm, the two-sided algorithm creates densely interconnected hubs. In a network with six nodes and

six links, the end-node algorithm would likely create a star-shaped topography, where the fittest node is a lender to most of the other nodes. The two-sided algorithm on the other hand would likely create a triangle-shaped topography, where the three fittest nodes are densely connected and the other nodes remain unconnected. The formation of vulnerable clusters of peripheral nodes is accordingly less likely and the core nodes have less connections with the periphery. Contagion is unlikely to spread far enough to trigger contagion within the core of the network. This is true even when the initially defaulted bank is a part of the core. It is also notable, that the self-averaging capabilities of the networks generated with the two-sided algorithm is quite low. The averages do not converge towards a smooth curve as quickly as the Erdős-Renyi or end-node networks, which makes it difficult to ascertain, how far the upper phase transition is pushed to the right when the shape parameter is increased.

We conducted a third set of numerical simulations, using a model calibrated with some key characteristics of the status quo of the Chinese financial network. For this set of simulations, we only iterate over the average degree. Figure (6) shows the simulation results for the different networks. We conduct two sets of simulations, one where a small bank initially defaults and one where a medium bank initially defaults. The first two graphs show the simulation results for a network with an Erdős-Renyi connection probability. The second row shows the simulations of the network generated by the two-sided fitness algorithm. The third row shows the network generated by the end-node fitness algorithm. In the case of the Erdős-Renyi connection probability, the difference between the default of a small bank and a medium bank for the stability of the system is relatively small, the fragile window ends at the same point and the frequency of systemic crisis is similar. It is notable, however, that the differences in size affect the extent of contagion. The presence of the large banks effectively prevents the system-wide spread of contagion. This feature, the role of the large banks as an effective stopgap for the occurrence of system-wide contagion, is repeated in the next two simulations.

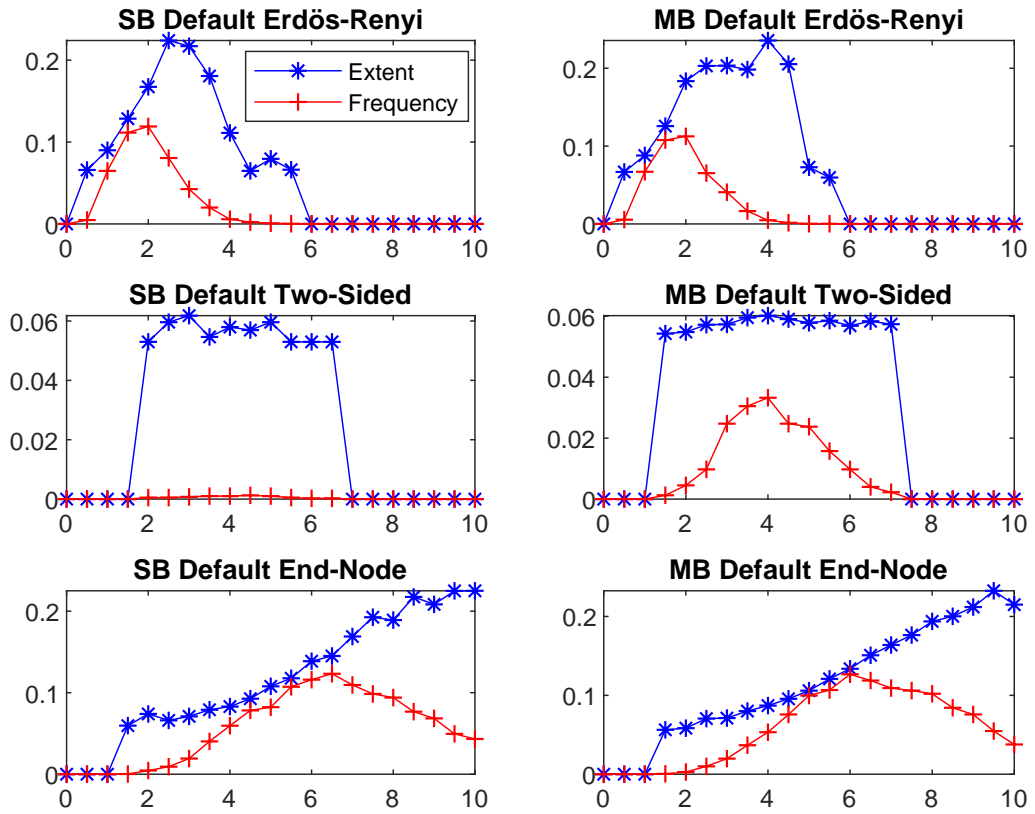


Figure 6: This graph shows the frequency and extent of contagion in the simulation of the model with Chinese characteristics over 4000 iterations. In the simulations on the left, a city commercial bank (SB) initially defaults and in the simulations on the right a joint-stock bank (MB) initially defaults. As before the curves with a star are the extent of contagion and the curves with crosses are the frequency of a systemic crisis.

It is particularly apparent in the simulation based on the two-sided algorithm. The massive concentration of connections and assets in the core effectively atomizes the size of vulnerable clusters. These clusters barely surpass the 5% threshold for a systemic crisis. Starting from the initial default of a medium sized bank does not alter this observation, but it significantly increases the frequency of systemic crisis. Through its own asset-based fitness, the medium sized bank is likely capable of drawing some smaller banks into its orbit. These smaller banks would be less well connected and therefore vulnerable to contagion. Once the connectivity of these smaller banks increases sufficiently, the vulnerable clusters vanish. Of the three different stylized topographies of the Chinese banking sector, the topography created by the end-node algorithm is the most vulnerable. While it is more stable than the Erdős-Renyi network when connectivity is low, it grows more vulnerable as connectivity increases. It stays in a fragile state longer than the two other topographies. There is little difference between the effect of an initial default of a small bank or that of a medium bank.

## 6 Concluding remarks

This paper analyzes how different assumptions about the topography of a network shape the extent and frequency of contagion within the network. In a first step, we used the framework provided by Newman, Strogatz and Watts (2001) and Gai and Kapadia (2010) to develop an analytical derivation for the effect that network topography has on the occurrence of contagion. Using a hidden variable model, we find that the occurrence of the phase transition of the network, the formation of a giant cluster of connected vulnerable banks, is highly dependent on the shape of the distribution of connection probabilities. The steeper this distribution becomes, the higher the average number of links has to become before a giant cluster of vulnerable banks forms with a high probability. The connection probabilities govern the network's topography. Our analytical derivation



therefore implies, that a more concentrated network will have its phase transitions at higher average number of links than a decentralized network.

We conduct numerical simulations of a generic model with different values for the shape parameter of the fitness distribution. We find that these simulations prove the results of the analytical derivation. The upper phase transition of networks with a steeper fitness distribution is further to the right than in a network with a less steep distribution, or a network with an Erdős-Renyi connection probability. This implies that more concentrated/ tiered networks are less fragile when connectivity is low. They however remain in a robust-yet-fragile state for higher levels of connectivity. The decentralized network becomes immune to contagion at lower levels of connectivity than the concentrated network. This is the effect of the formation of links between poorly connected peripheral nodes in the concentrated networks. At low levels of connectivity these networks have very few, if any, connections between peripheral nodes. When connectivity increases, links between peripheral nodes are established. Because of the sparseness of intra-periphery connections, these connected peripheral nodes will likely be poorly diversified and therefore vulnerable to contagion. This leads to the potential formation of vulnerable clusters of peripheral banks in concentrated networks at higher levels of connectivity.

A similar observation can be made for the simulation of a model with Chinese characteristics. The model based on the sizes of the bank balances is a slightly concentrated network, with the five largest state-controlled banks at its center. This model is more robust to contagion. The large well-capitalized banks operate as an efficient stopgap for the spread of contagion. However, the upper phase transition is also further to the right than in a decentralized model with Chinese characteristics. We also find that the extent of contagion in an end-node network with Chinese characteristics increases with connectivity. This type of network is the most vulnerable to a growth in intra-peripheral connectivity.

We conclude accordingly that there may be a hidden riskiness to more concentrated networks. The existence of large connected clusters of otherwise sparsely connected peripheral banks can become a problem for network stability. If these clusters become large enough, they may endanger the stability of the entire network. This danger increases with the relative weight of the peripheral banks. As the Chinese example shows, a significant share of the assets of the financial system has to be allocated in peripheral banks to allow for system-wide contagion. Vulnerable peripheral clusters are encountered in more concentrated networks at higher degrees of connectivity than in decentralized networks. This is especially visible in the networks created by the end-node algorithm. Financial innovation, such as syndicated loans and other new financial instruments, may facilitate a greater role for peripheral banks. A deeper role for the peripheral banks in the interbank market could create a situation, where the financial system is robust-yet-fragile and vulnerable to large default cascades.

We conclude additionally, that the Chinese financial network is facing the same hidden dangers as a generic model. The privileged position of the five larges banks acts for the time being as an effective stopgap, which limits the possible extent of contagion and the potential for the occurrence of a contagion cascade. The trend of a fading market dominance of these banks however may reduce this stopgap function and increase the danger of system wide contagion. This is especially relevant in the case where less well capitalized banks with a higher investment in the interbank markets (like for example some of the medium sized banks) start to take over more of the liquidity providing role of the largest banks. While the default of a single small city commercial bank is of little concern in the financial network of today, it may become a concern when deeper integration forges lager clusters of vulnerable banks. Better interbank market access and the development of the financial market should therefore be accompanied by a reinforced effort to establish sound business practices in all of China's commercial banks.

## Bibliography

- Acemoglu, Daron, Asuman Ozdaglar and Alireza Tahbaz-Salehi. 2015. “Systemic Risk and Stability in Financial Networks.” *American Economic Review* 105(2).
- Allen, Franklin and Douglas Gale. 2000. “Financial Contagion.” *Journal of Political Economy* 108(1).
- Amini, Hamed, Rama Cont and Andreea Minca. 2016. “RESILIENCE TO CONTAGION IN FINANCIAL NETWORKS.” *Mathematical Finance* 26(2).
- Bianconi, Ginestra and Albert-Laszlo Barabasi. 2001. “Competition and multiscaling in evolving networks.” *Europhysics Letters* 54(4).
- Boguñá, Marián and Romualdo Pastor-Satorras. 2003. “Class of correlated random networks with hidden variables.” *Phys. Rev. E* 68.
- Caldarelli, Guido, Andrea Capocci, Paolo De Los Rios and Miguel A. Munoz. 2002. “Scale-Free Networks from Varying Vertex Intrinsic Fitness.” *Physical Review Letters* 89(25).
- Castiglionesi, fabio and Noemi Navarro. 2019. “(In)Efficient Interbank Networks.” *Journal of Money, Credit and Banking* n/a(n/a).
- Cont, Rama, Amal Moussa and Edson B. Santos. 2013. *Network Structure and Systemic Risk in Banking Systems*. Cambridge University Press p. 327–368.
- Eisenberg, Larry and Thomas H. Noe. 2001. “Systemic Risk in Financial Systems.” *Management Science* 47(2).
- Financial Stability Analysis Group of the PBoC. 2019. “China Financial Stability Report 2019.” *China Financial Stability Report* .
- Gai, Prasanna, Andrew Haldane and Sujit Kapadia. 2011. “Complexity, concentration and contagion.” *Journal of Monetary Economics* 58(5).
- Gai, Prasanna and Sujit Kapadia. 2010. “Contagion in financial networks.” *Proceedings of the Royal Society* 466(A).
- Masi, Gabriele De Luca De, Giulia Iori and Guido Caldarelli. 2006. “A fitness model for the Italian Interbank Money Market.” *Physical Review E* 74.
- Newman, M. E. J., S.H. Strogatz and D.J. Watts. 2001. “Random graphs with arbitrary degree distributions and their applications.” *Physical Review E* 64.
- Newman, Mark E. J. 2002. *Random Graphs as Models of Networks*.
- Nier, Erlend, Jing Yang, Tanju Yorulmazer and Amadeo Alentorn. 2008. “Network models and financial stability.” *Bank of England Working Papers* 346.

- Reserve Bank of Australia. 2017. "The Chinese Interbank Repo Market." *Reserve Bank of Australia Bulletin* .
- Reserve Bank of Australia. 2019. "Small Banks in China." *RBA Statement on Monetary Policy* .
- Söderberg, Bo. 2003. "Random Graph Models with Hidden Color." *Acta Physica Polonica B* 34(10).
- Sun, Lixin. 2018. "Financial Networks and Systemic Risk in China's Banking System." *MPRA Paper* .
- Xia, Le. 2020. "Lessons from China's past banking bailouts." *Bank of Finland Policy Brief* 3.
- Xian, Gu and Yun Lu. 2019. "The Unintended Consequences of Regulation: Evidence from China's Interbank Markets." *HKIMR Working Paper* 06.